AC
FHI

LECTURE SERIES
HETEROGENEOUS CATALYSIS

Powder X-ray and neutron diffraction

Lecture series: Modern Methods in Heterogeneous Catalysis Research

Malte Behrens, FHI-AC
behrens@fhi-berlin.mpg.de

Outline

- Fundamentals of diffraction
  - What can we learn from a diffraction experiment?
- X-ray diffraction
  - Powder techniques
  - Phase analysis
  - Refinement of XRD data
    - Line profile analysis
    - Rietveld refinement
- Neutron diffraction
  - Neutrons vs. X-ray

Fundamentals of diffraction

- Transverse plane waves from different sources can “interfere” when their paths overlap
- constructive interference (in phase)
- destructive interference (out of phase), completely destructive for the same amplitude and wavelength
- partially destructive for different amplitudes and wavelengths

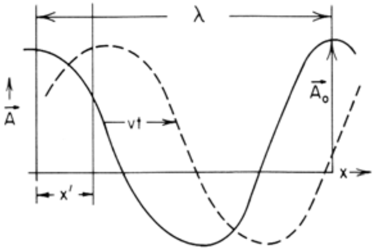

FIG. 3-1. A cosine wave moving to the right.

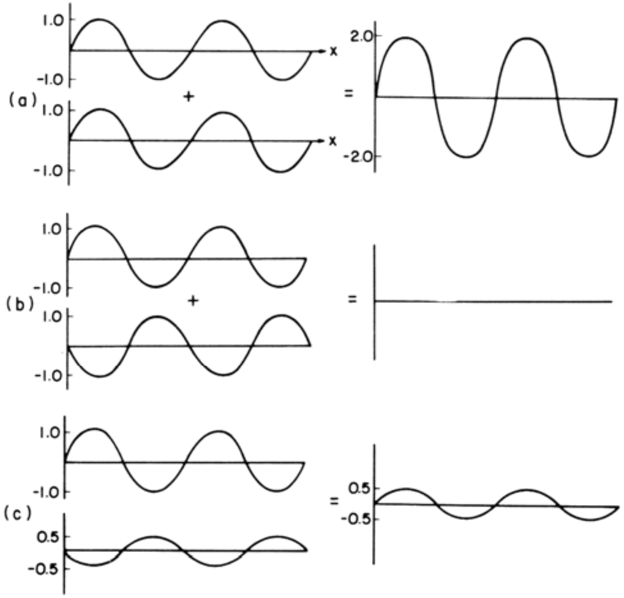

FIG. 3-2. Interference between two waves. Both waves are assumed to have the same maximum amplitude (unity) except in (c) and the same wavelength in all cases. (a) Constructive interference; (b) complete destructive interference; (c) partial destructive interference.

Diffraction experiments

- Interference patterns can be produced at diffraction gratings (regularly spaced "slits") for d ≈ λ
- Waves from two adjacent elements (1) and (2) arrive at (3) in phase if their path difference is an integral number of wavelengths
- Kinematic theory of diffraction:
  - R >> d: contributions of each beam can be taken as a plane traveling wave
  - Conservation of energy in the scattering process
  - A once-scattered beam does not re-scatter
- Periodically arranged atoms (crystals) act as diffractions gratings for radiation 0.6 ≤ λ ≤ 1.9 Å (M. von Laue, W. Friedrich, P. Knipping, 1912)

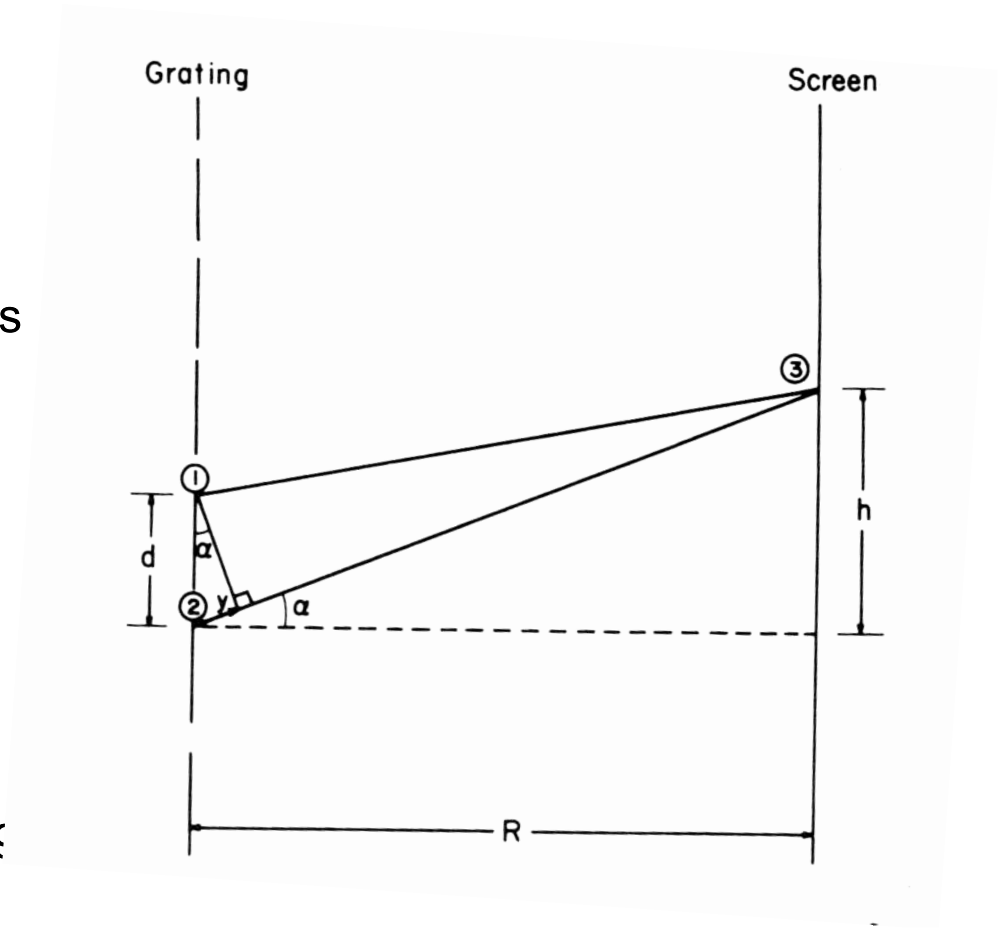

The Bragg equation

- GE = EH = d sinθ
- $n\lambda = 2d \sin\theta$ (Sir W.L. Bragg)
  - $2d < \lambda$: no diffraction
  - $2d > \lambda$: different orders of diffractions (n= 1, 2, …) at different angles
  - $2d >> \lambda$: 1st order reflection too close to direct beam

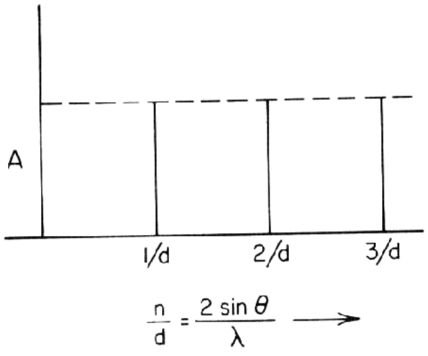

FIG. 3-5. Amplitude versus 2 sin θ/λ.

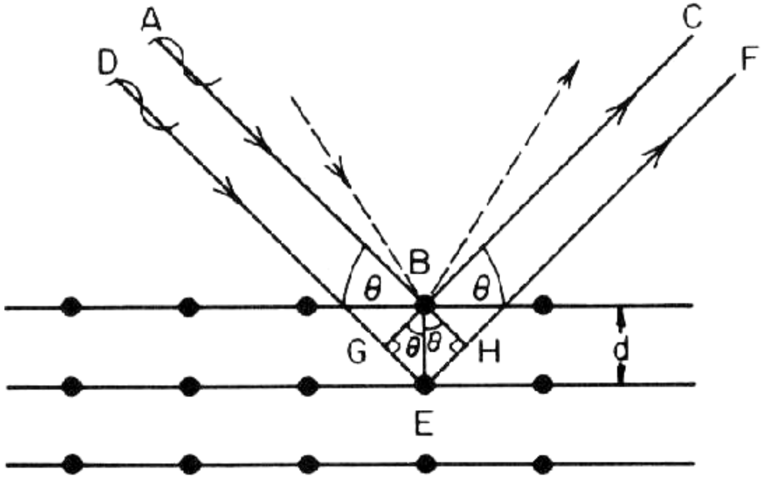

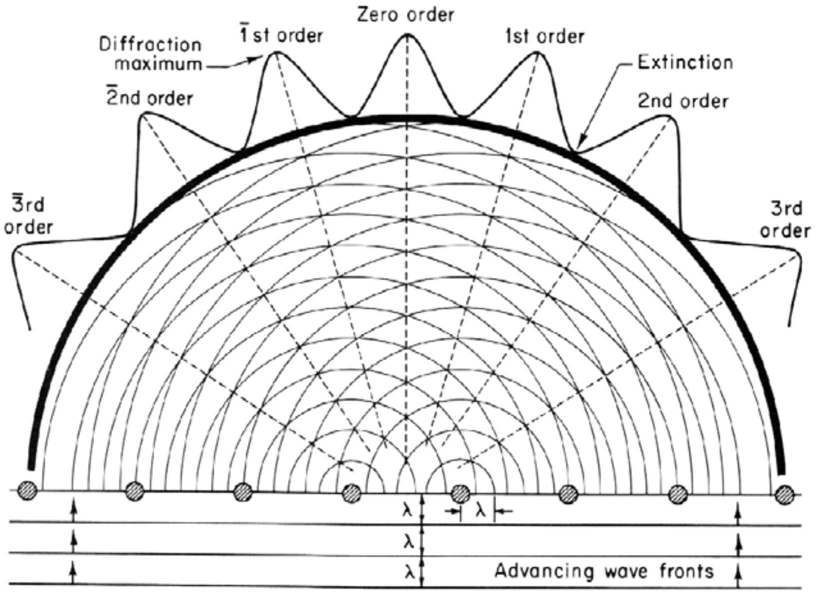

Fig. 3-1. Reinforced scattering by a regularly spaced row of atoms.

Diffraction from planes of atoms

- Interposition of the same types of atoms at d/4
  - n=1: path difference between planes A and B is λ, between A and a it is $\lambda/4$ → partially destructive interference
  - n=2: path difference between A and B is 2λ, between A and a it is $\lambda/2$ → complete destructive interference, "peak" eliminated
  - n=3: again partially destructive interference
  - n=4: all planes "in phase"
- Different atoms at d/4 than in A and B
  - no complete vanishing of intensity for n=2

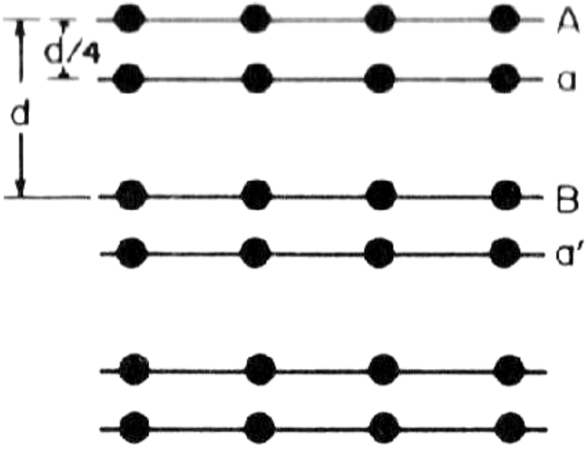

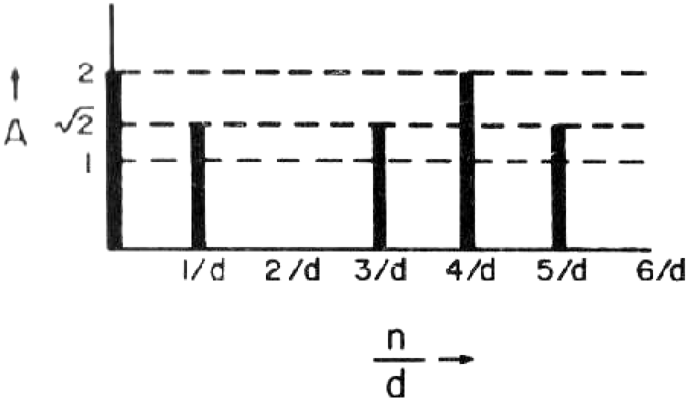

Diffraction from a real crystal structure

- Pioneering study of Sirs W.H. and W.L. Bragg, 1913
- NaCl (cubic), measurement of amplitude of scattered X-ray from (100), (110) and (111) by tilting the crystal
- The alternating amplitude in (c) indicates the alternation of Na and Cl layers in (111)

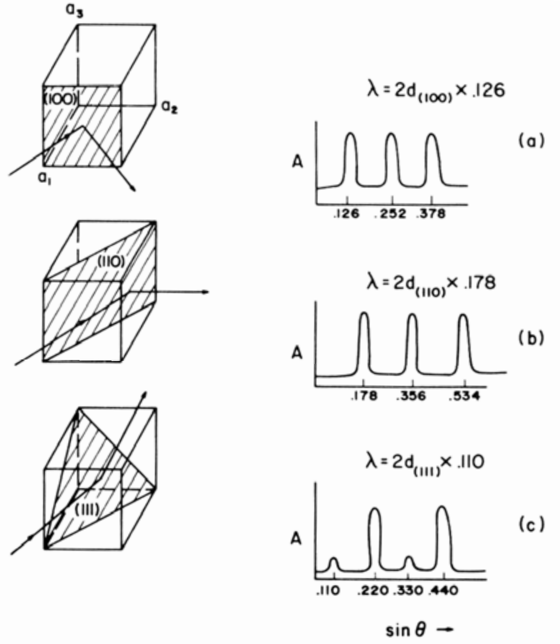

FIG. 3-9. Diffraction from different faces of an NaCl crystal. [After Bragg, W. H., *Proc. Roy. Soc., London* **A89** 246 (1913).]

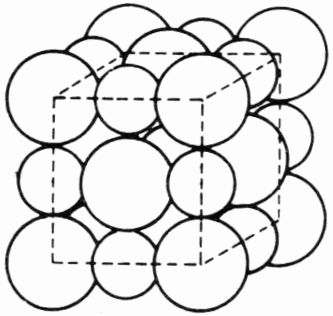

(c) NaCl: $F\frac{4}{m}\bar{3}\frac{2}{m}$

$a = 5.64$ Å
$r_{Na^+} = 0.97$ Å
$r_{Cl^-} = 1.81$ Å
4 "molecules"/cell

Scattered intensity and crystal structure

- Total scattering power of a reflection

$$P = I_0 \frac{V \cdot \lambda^3 \cdot m \cdot F^2}{4 \cdot v_a^2} \left(\frac{1 + \cos^2 2\theta}{2 \cdot \sin \theta} \right) \left(\frac{e^4}{m_e^2 c^4} \right)$$

  - m: multiplicity, v_a: volume of unit cell, V: illuminated volume of powder sample

- The structure factor F_{hkl}
  - $I_{hkl} \sim |F_{hkl}|^2$
  - $F_{hkl} = \Sigma f_{jT} \exp 2\pi i(h \cdot x_j + k \cdot y_j + l \cdot z_j)$
  - f_{iT}: atomic scattering factor

Atomic scattering factor

- X-ray photons interact with the electron clouds of an atom
- electron clouds are not points in space, but possess a finite size of the same magnitude as the X-ray wavelength
- electrons are spread in space and consequently not all are scattering in phase, the scattering amplitude will vary with 2θ
- atomic scattering factor (ratio of the amplitude scattered by an atom to that scattered by a single electron) fall off with (sinθ)/λ
- As a consequence, the Bragg peaks at higher angles will generally exhibit a lower intensity compared to those at lower angels

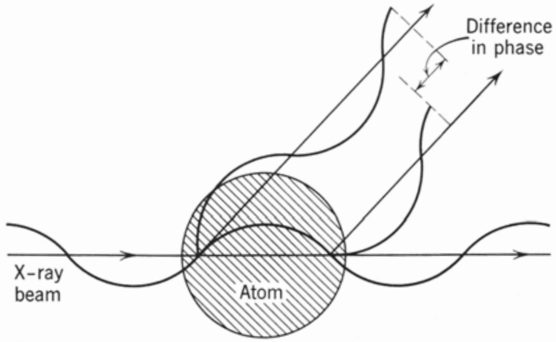

Fig. 3-14. Phase difference in scattering from different parts of an atom.

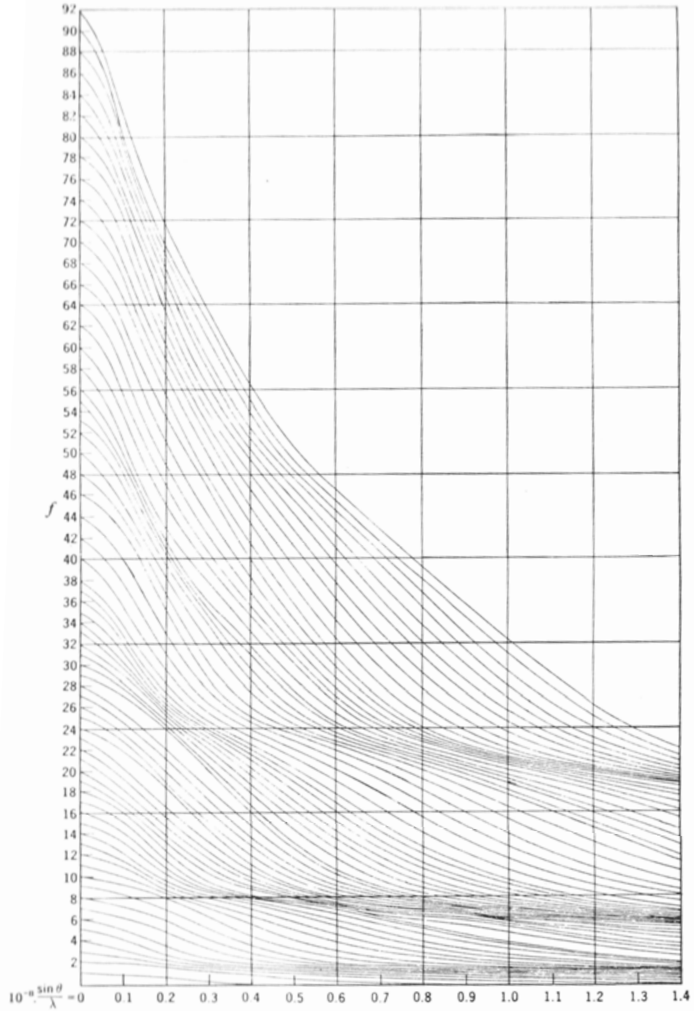

Fig. 1.2 The X-ray atomic scattering factor, *f*, shown as a function of (sin θ)/λ for neutral atoms. The numbers along the ordinate are the atomic numbers, *Z*. (From Buerger 1942.)

What can we learn from a diffraction experiment

- Are there peaks? (Crystallinity)
- Which crystalline phases are present? (Phase identification, database of fingerprint patterns)
- How many crystalline phases are present? (Homogeneity)
- Relative amount of phases? (Quantitative phase analysis)
- Crystal structure refinement
- Size, strain

X-ray diffraction

- X-ray have wavelengths around 1 Å (≈ d) (W.C. Röntgen, 1895)
- Easily produced in X-ray tube

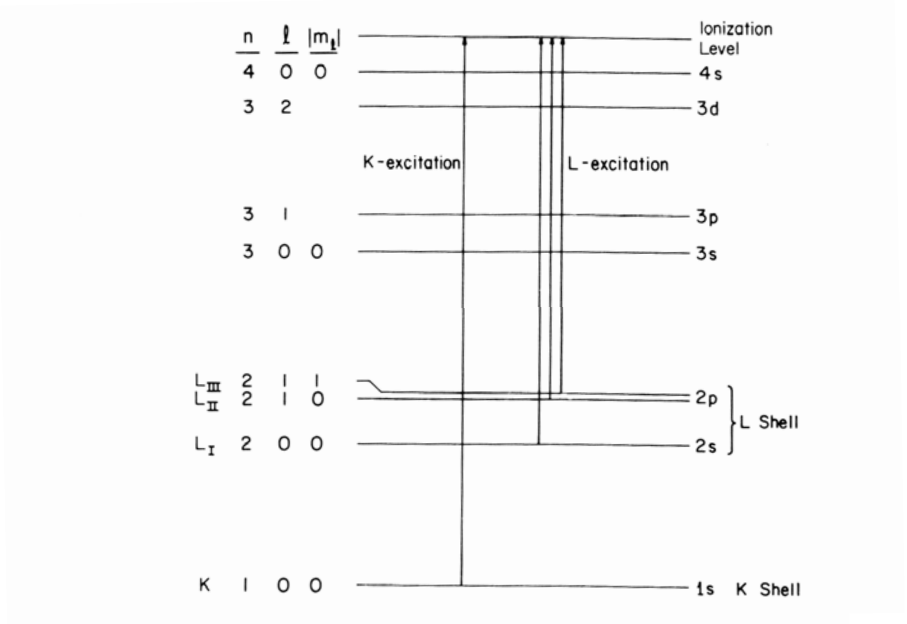

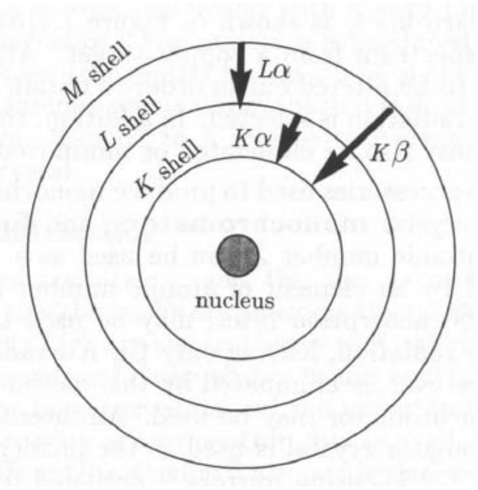

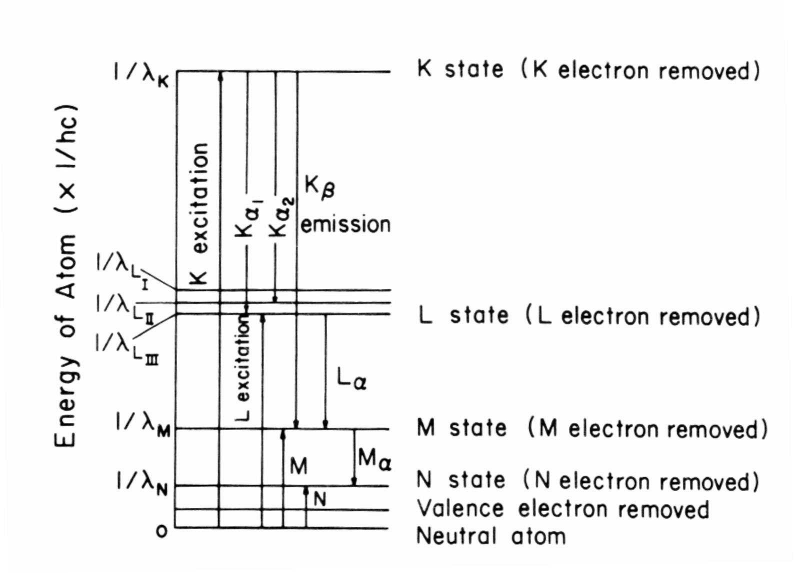

X-ray tubes

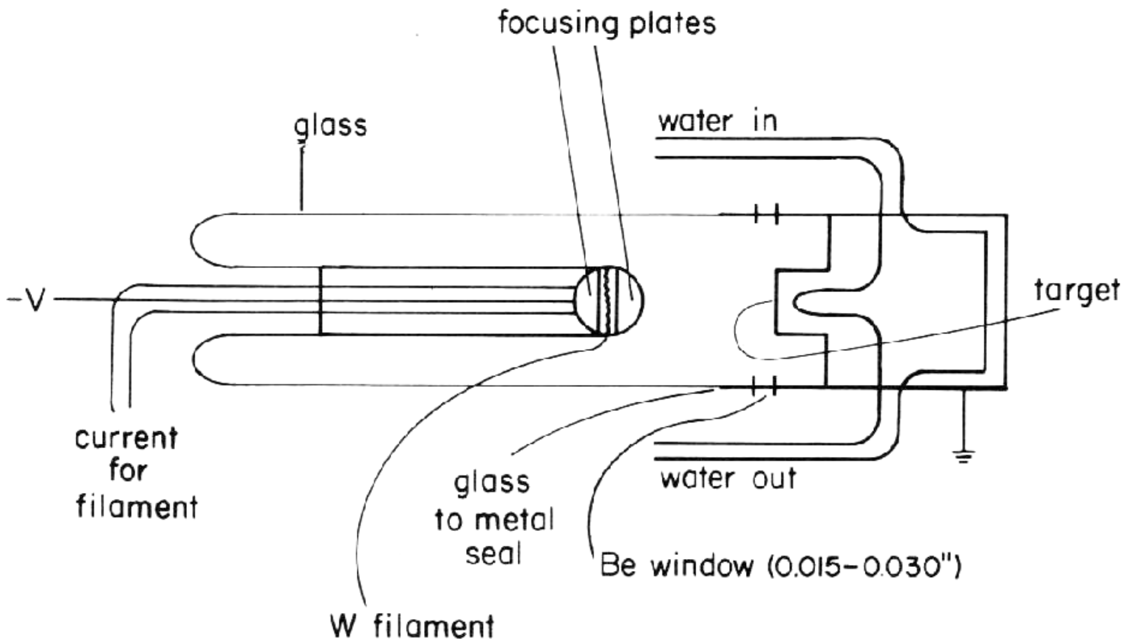

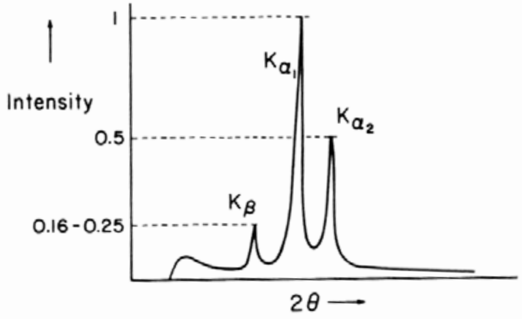

FIG. 4-6. The white and characteristic spectrum from an x-ray tube. The K_{α_1} transition has a higher energy than K_{α_2} and therefore a smaller wavelength. Hence the K_{α_1} peak occurs at a smaller 2θ since Bragg's law requires $\lambda = 2d \sin\theta$.

Geometry of diffractometers

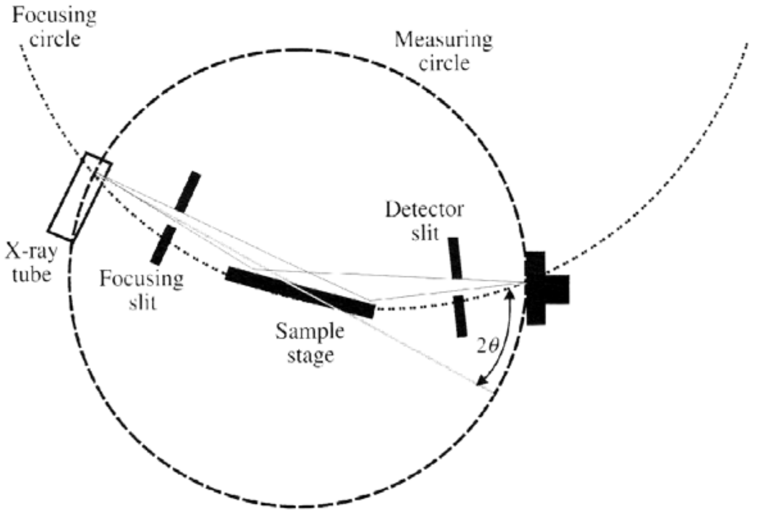

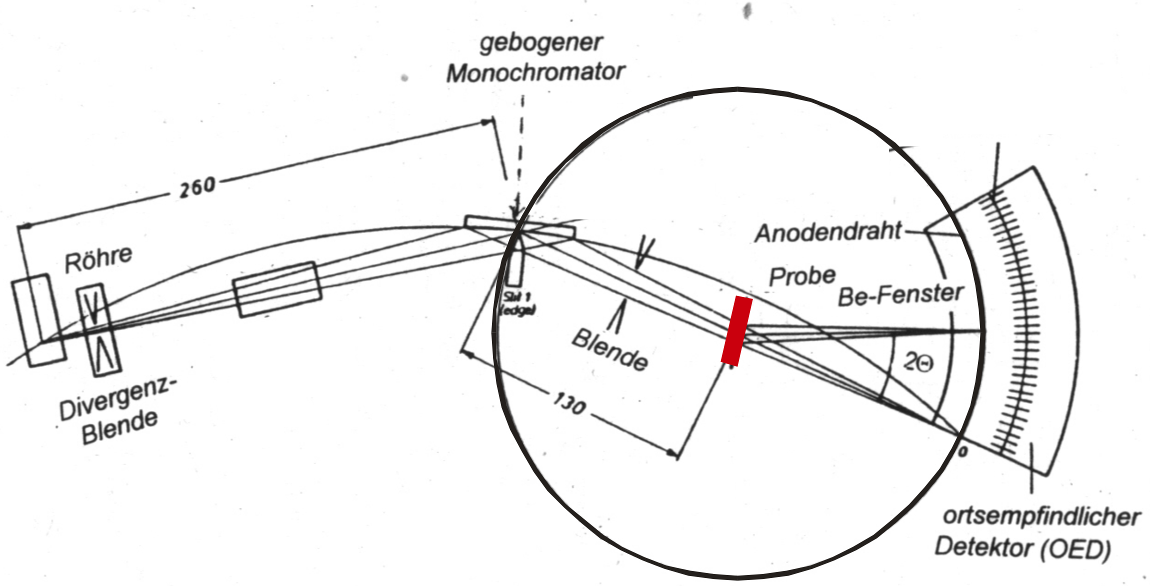

- Reflection geometry
  - θ-2θ
  - θ-θ
- Transmission geometry

Powder XRD patterns

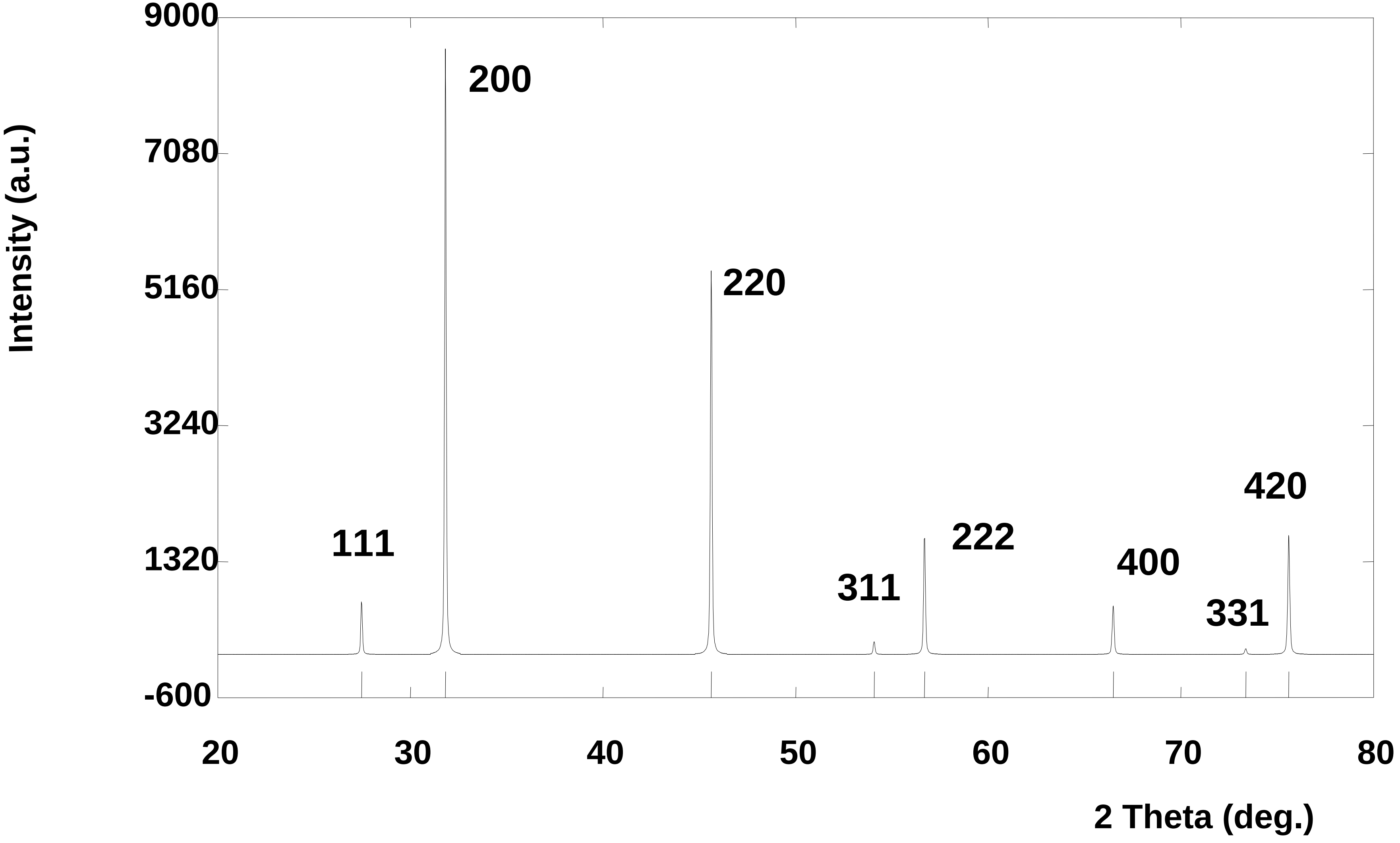

NaCl, Cu Kα

Kα2 contribution

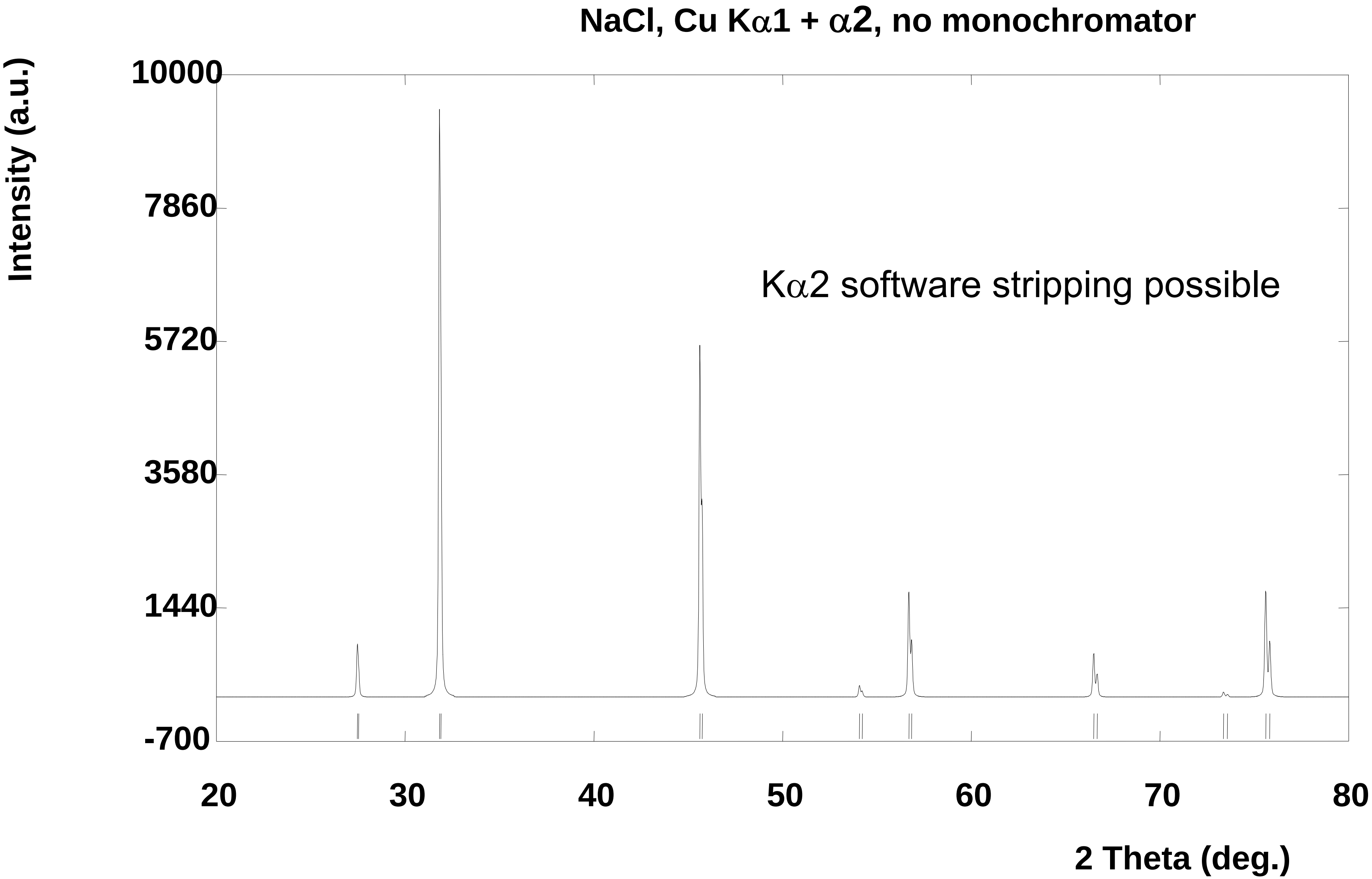

Kα2 software stripping possible

Effect of wavelength

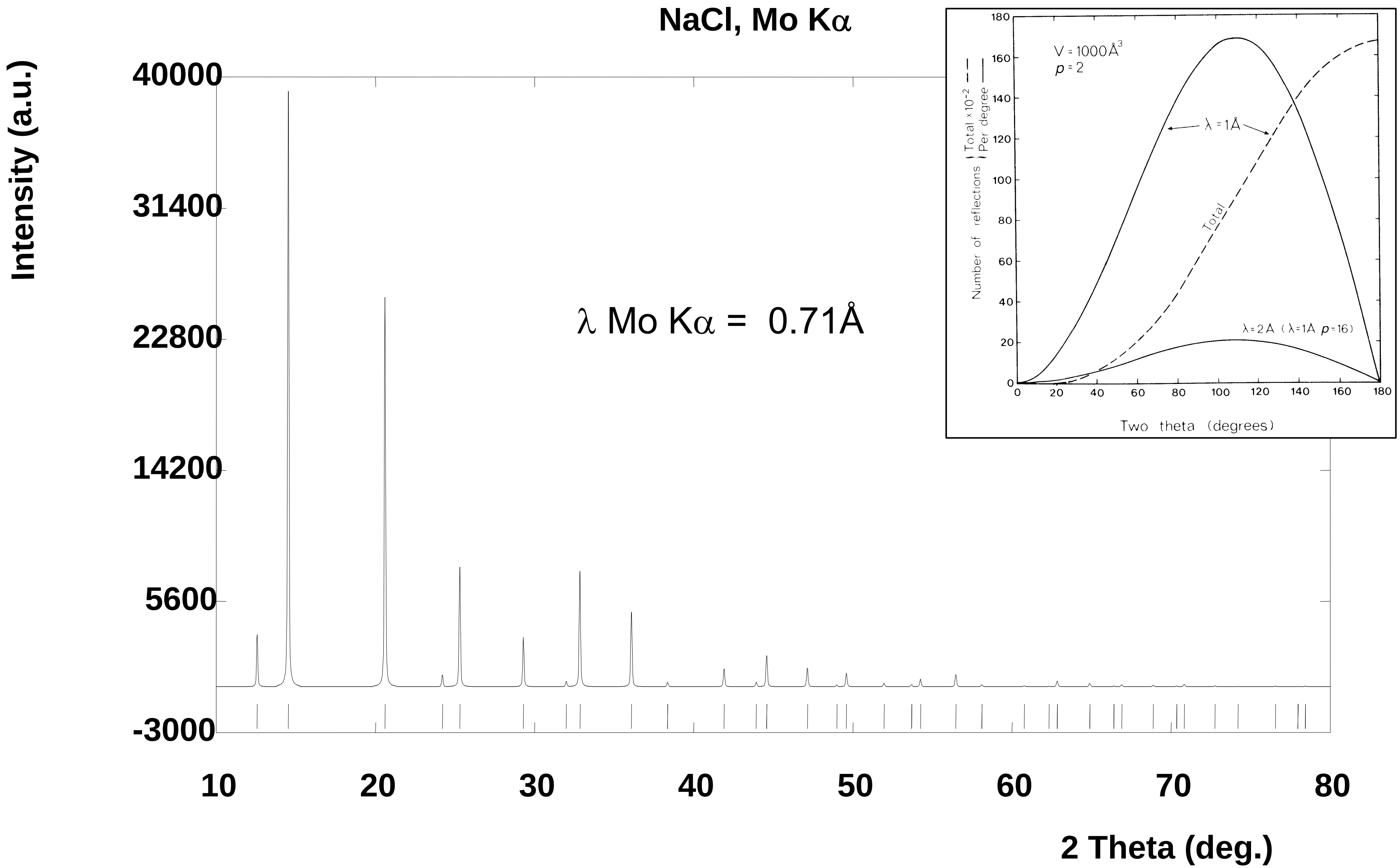

NaCl, Mo Kα

λ Mo Kα = 0.71Å

Information content of an idealized diffraction pattern

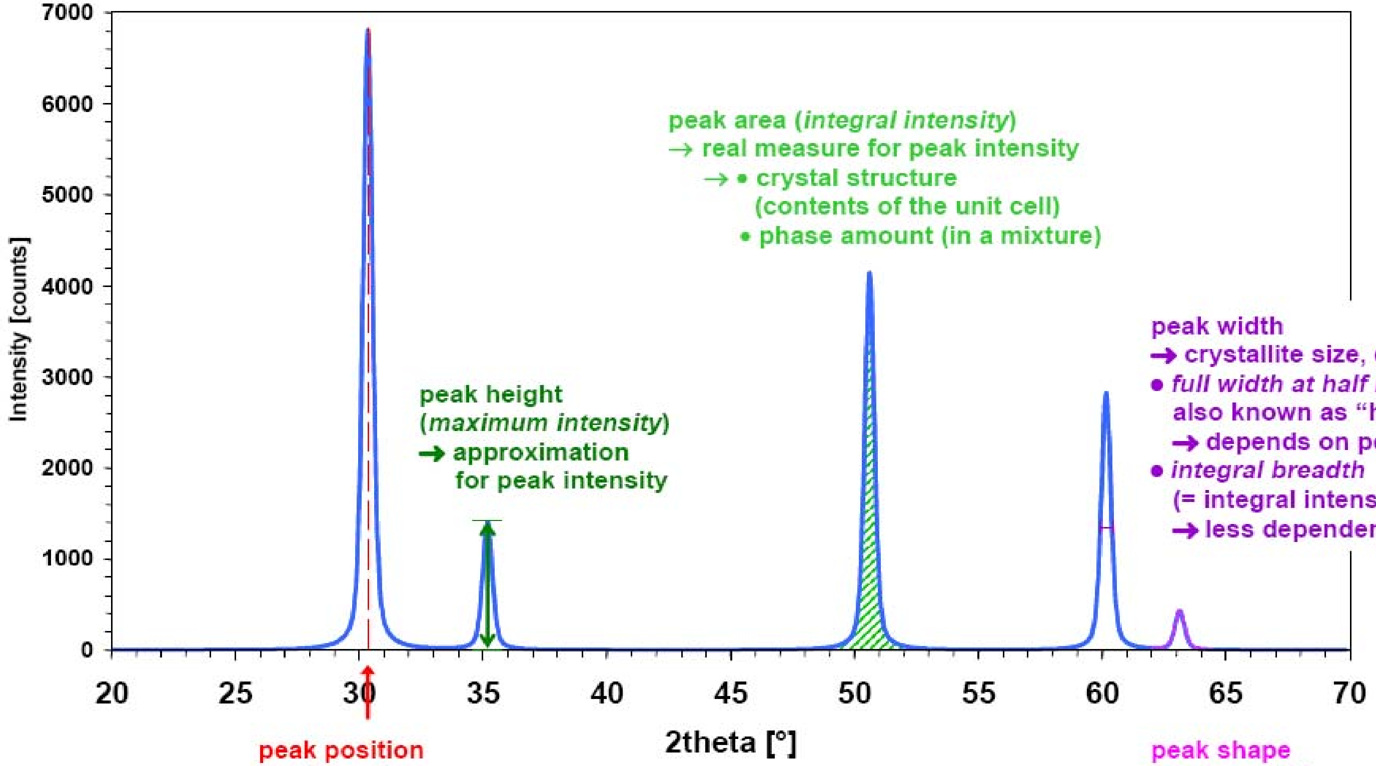

peak area (*integral intensity*)
→ real measure for peak intensity
→ • crystal structure
(contents of the unit cell)
• phase amount (in a mixture)

peak height
(*maximum intensity*)
➔ approximation
for peak intensity

peak width
➔ crystallite size, defects (strain, disorder)
• *full width at half maximum* (FWHM),
also known as "half width"
➔ depends on peak profile!
• *integral breadth*
(= integral intensity / maximum intensity)
➔ less dependent on peak profile

peak position
➔ d-spacing
➔ lattice parameters
(metrics of the unit cell)

peak shape
(*peak profile*)
➔ crystallite size, defects
(strain, disorder)

Phase analysis

- Peak positions and intensities are compared to a patterns from the powder diffraction file (PDF) database
- Generally, ALL peaks found in a PDF pattern must also be seen in in the diffractogram, otherwise it is not a valid match
- Possible exceptions:
  - Small peaks may be not detectable if the noise level is too high
  - Missing peaks may be the result of a very strong preferred orientation effect (intensities systematically hkl-dependent)
  - “Missing” peaks may be the result of anisotropic disorder (FWHMs systematically hkl-dependent)
  - Very small residual peaks may be artifacts resulting from spectral impurities (other wavelengths, e.g. Kβ, W L)
  - The peaks are real, but they belong to the reference compound, not an impurity. It may be that your diffraction pattern is “better” in terms of signal/noise ratio than the (possibly old) PDF pattern. After all, the diffractometers have improved with time (Rietveld check required)
- Systematic shifts of peak position might be due to thermal expansion (check PDF entry) or different composition

F.Girgsdies

X-ray Powder Diffraction in Catalysis

Possibilities of XRD analysis: qualitative analysis

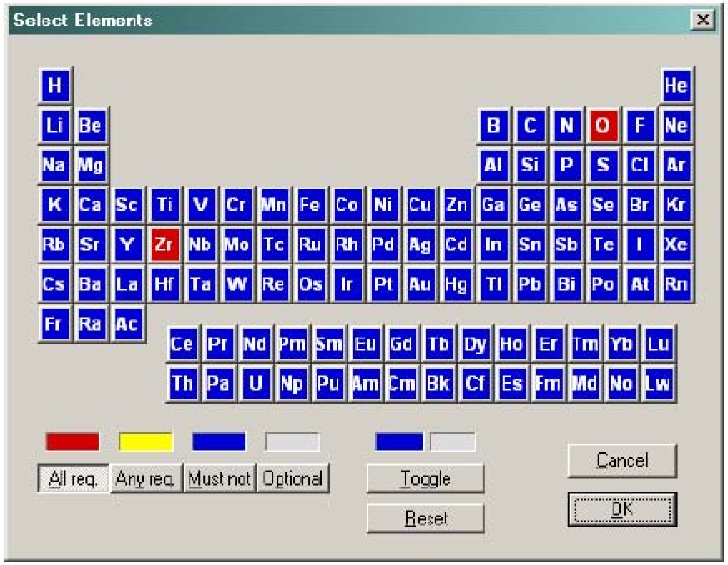

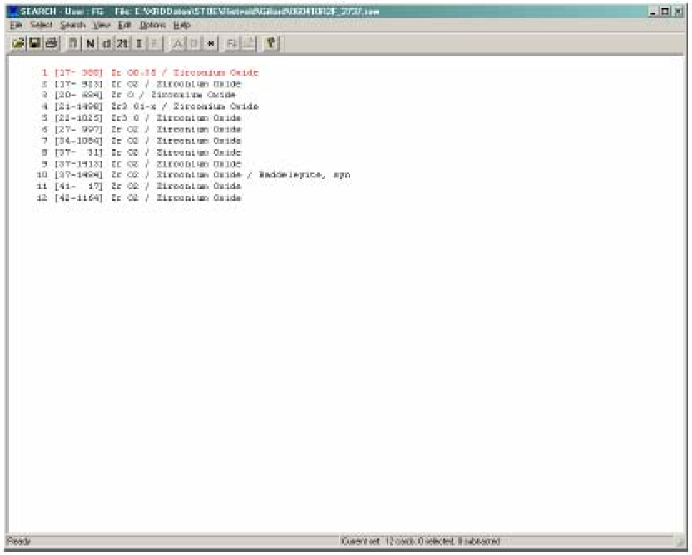

```
 1 [17- 385] Zr O0.35 / Zirconium Oxide
 2 [17- 923] Zr O2 / Zirconium Oxide
 3 [20- 684] Zr O / Zirconium Oxide
 4 [21-1498] Zr3 O1-x / Zirconium Oxide
 5 [22-1025] Zr3 O / Zirconium Oxide
 6 [27- 997] Zr O2 / Zirconium Oxide
 7 [34-1084] Zr O2 / Zirconium Oxide
 8 [37-  31] Zr O2 / Zirconium Oxide
 9 [37-1413] Zr O2 / Zirconium Oxide
10 [37-1484] Zr O2 / Zirconium Oxide / Baddeleyite, syn
11 [41-  17] Zr O2 / Zirconium Oxide
12 [42-1164] Zr O2 / Zirconium Oxide
```

Ready   Current set: 12 cards 0 selected, 0 subtracted

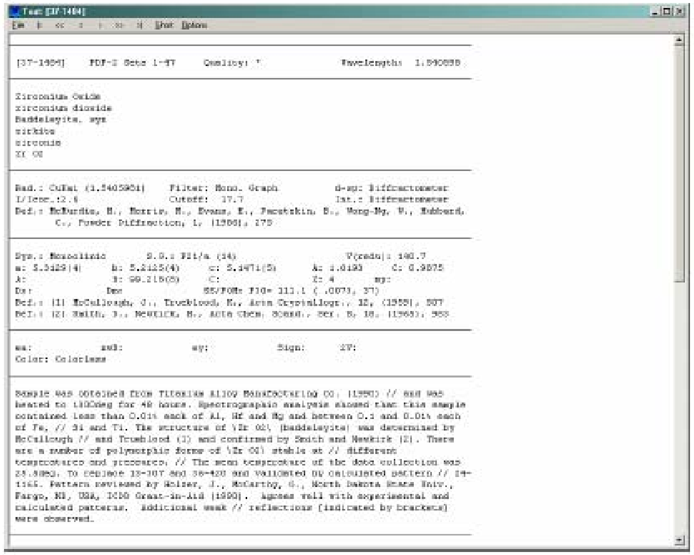

```
[37-1484]     PDF-2 Sets 1-47     Quality: *          Wavelength:  1.540598

Zirconium Oxide
zirconium dioxide
Baddeleyite, syn
zirkite
zirconia
Zr O2

Rad.: CuKa1 (1.5405981)    Filter: Mono. Graph          d-sp: Diffractometer
I/Icor.:2.6                Cutoff:  17.7                Int.: Diffractometer
Ref.: McMurdie, H., Morris, M., Evans, E., Paretzkin, B., Wong-Ng, W., Hubbard,
      C., Powder Diffraction, 1, (1986), 275

Sys.: Monoclinic       S.G.: P21/a (14)                  V(redu): 140.7
a: 5.3129(4)     b: 5.2125(4)     c: 5.1471(5)      A: 1.0193     C: 0.9875
A:               B: 99.218(8)     C:                Z: 4          mp:
Dx:              Dm:              SS/FOM: F30= 111.1 ( .0073, 37)
Ref.: (1) McCullough, J., Trueblood, K., Acta Crystallogr., 12, (1959), 507
Ref.: (2) Smith, D., Newkirk, H., Acta Chem. Scand., Ser. B, 18, (1965), 983

ea:            nwB:             ey:              Sign:      2V:
Color: Colorless

Sample was obtained from Titanium Alloy Manufacturing Co. (1950) // and was
heated to 1100Cdeg for 48 hours. Spectrographic analysis showed that this sample
contained less than 0.01% each of Al, Hf and Mg and between 0.1 and 0.01% each
of Fe, // Si and Ti. The structure of \Zr O2\ (baddeleyite) was determined by
McCullough // and Trueblood (1) and confirmed by Smith and Newkirk (2). There
are a number of polymorphic forms of \Zr O2\ stable at // different
temperatures and pressures. // The mean temperature of the data collection was
25.8Cdeg. To replace 13-307 and 36-420 and validated by calculated pattern // 24-
1165. Pattern reviewed by Holzer, J., McCarthy, G., North Dakota State Univ.,
Fargo, ND, USA, ICDD Grant-in-Aid (1990).  Agrees well with experimental and
calculated patterns.  Additional weak // reflections (indicated by brackets)
were observed.
```

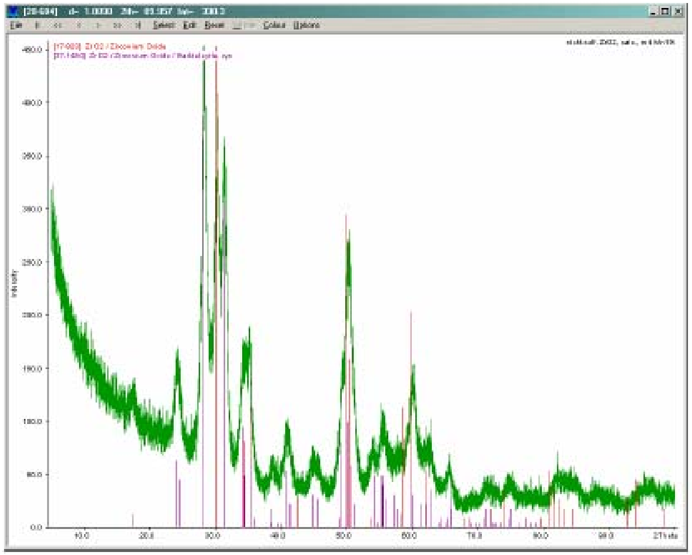

Refinement of PXRD data

- Refinement of powder XRD data can yield
  - crystal structure of the sample (model required)
  - quantitative phase analysis

    → Rietveld method (H.M. Rietveld, 1967)

  - information on size and strain

    → Line profile analysis

Line profile analysis

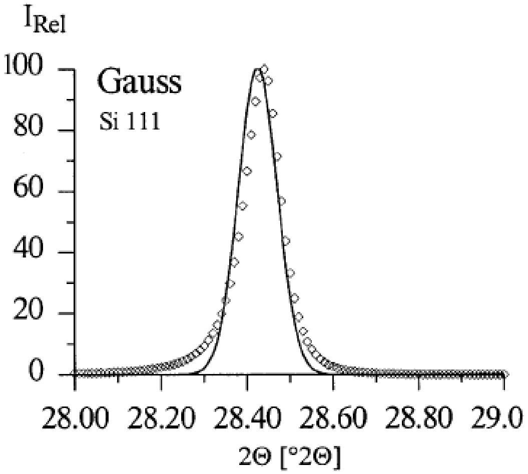

a)

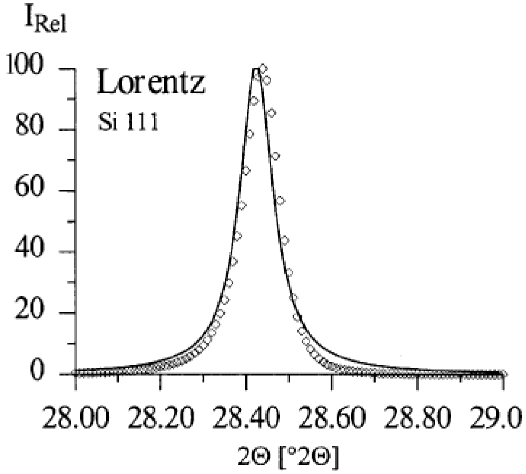

b)

- Fitting of a suitable profile function to the experimental data
  - Gauss, Lorentz, Pseudo-Voigt, Pearson-VII
- No structural model
- Parameters for each reflection:
  - angular position (2θ)
  - maximal intensity I_{max}
  - integral intensity A
  - FWHM or integral breadth $\beta = A / I_{max}$
  - profile paramter (P7: m, pV: η)
- Patterns of high quality and with low overlap of peaks are required

Instrumental contribution

- Line width dominated by beam divergence and flat-sample-error (low 2θ), slits (medium 2θ) and wavelength distribution in spectrum of XRD tube (high 2θ)
- Peaks of standard sample (large crystals, no strain, similar to sample, same measurement conditions) can be extrapolated by fitting a Cagliotti function

$$\mathrm{FWHM}^2 = U \tan^2\theta + V \tan\theta + W$$

Instrumental resolution function

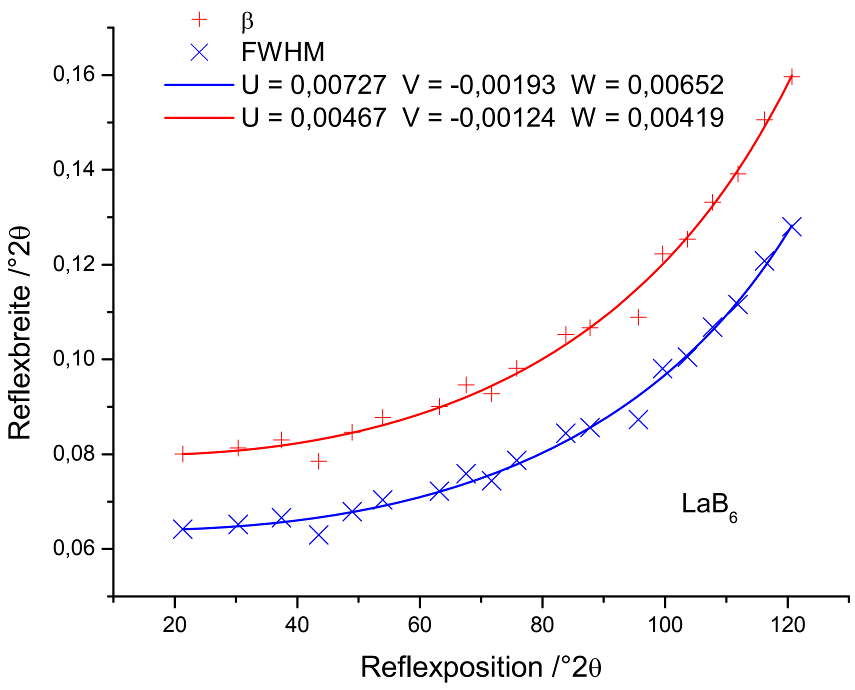

Sample line broadening

- Size effect
  - incomplete destructive interference at $\theta_{Bragg} \pm \Delta\theta$ for a limited number of lattice planes
  - detectable for crystallites roughly < 100 nm
  - no 2θ dependence

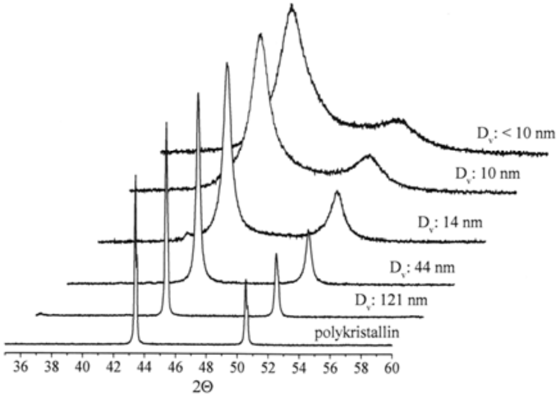

Abb. 16: 111- und 200-Reflex von Kupferproben mit unterschiedlicher Teilchengröße

- Strain effect
  - variation in d
  - introduced by defects, stacking fault, mistakes
  - depends on 2θ

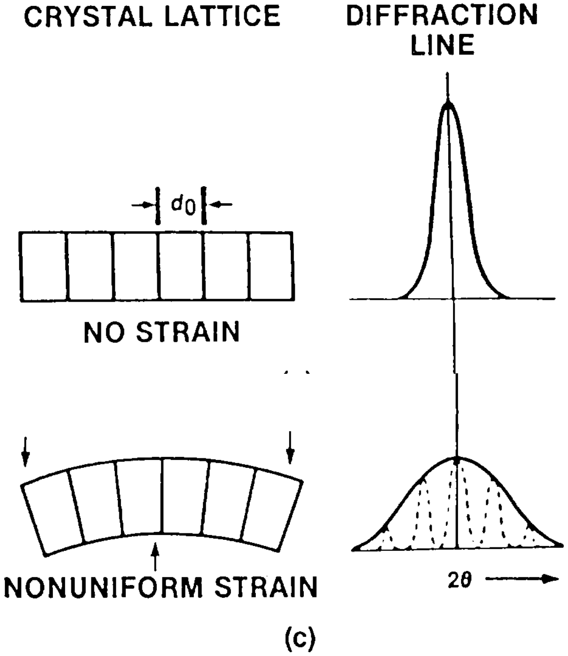

Scherrer equation

- Determination of size effect, neglecting strain (Scherrer, 1918)
- Thickness of a crystallite $L = N\, d_{hkl}$

  $L_{hkl} = k\, \lambda / (\beta \cos\theta)$,

  β has to be corrected for instrumental contribution:

  $\beta^2 = \beta^2_{obs} - \beta^2_{standard}$
  (for Gaussian profiles)

  – k: shape factor, typically taken as unity for β and 0.9 for FWHM
- Drawbacks: strain not considered, physical interpretation of L, no information on size distribution

Pattern decomposition

- β_{size}, β_{strain} and β_{instr} contribute to β_{obs}
- Software correction for β_{instr} from IRF
- Reciprocal quantities for each reflection
  - $\beta^* = \beta \cos \theta / \lambda$
  - $|d^*| = 1 / d = 2 \sin \theta / \lambda$

Wiliamson-Hall analysis

- Indexed plot of β* vs d*
  - Horizontal line: no strain, isotropic size effect
  - Horizontal lines for higher order reflections: no strain, anisotropic size effect
  - Straight line through the origin: isotropic strain
  - Straight line for higher order reflections but different slopes: anisotropic strain

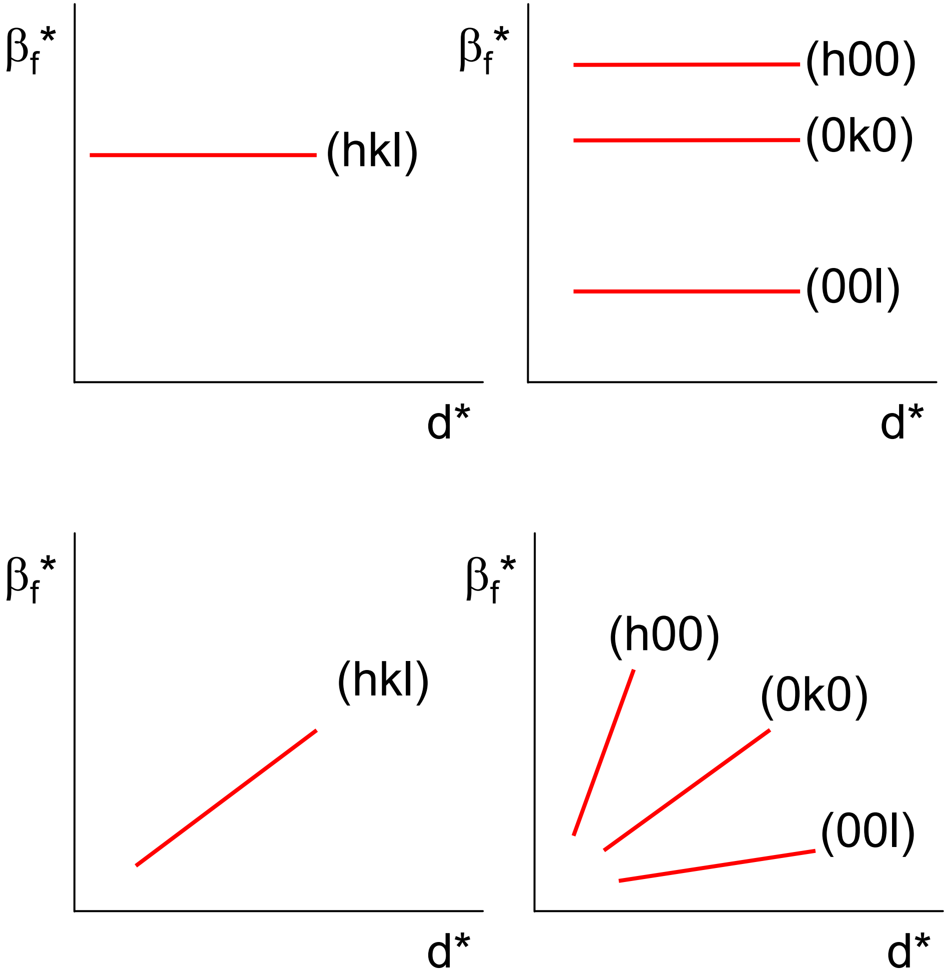

Example: ZnO

- ZnO obtained by thermal decomposition of $Zn_3(OH)_4(NO_3)_2$

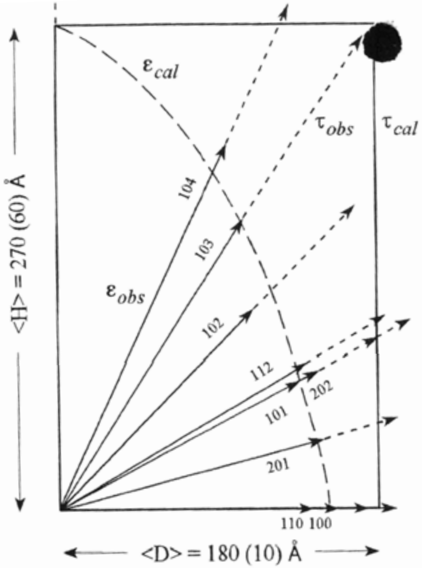

Fig. 28.8. Section through the 'average' cylinder (τ_{cal}) used to model the form of the crystallites of the ex-hydroxide-nitrate ZnO sample. ⟶: observed apparent size ε_{obs}, – – – –→: actual observed size τ_{obs} in the direction *hkl*, the dotted curve is the loci of the calculated apparent sizes (from Langford *et al.*, 1993).

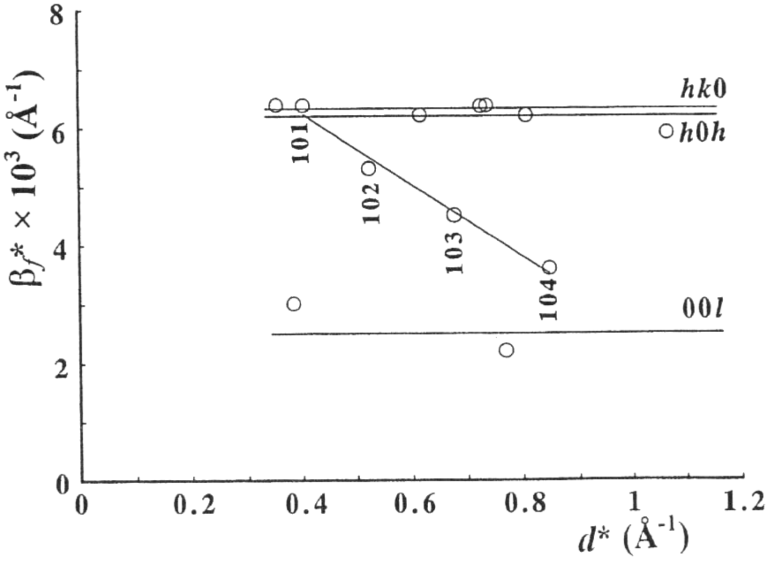

Fig. 28.7. Williamson–Hall plot for strain-free ex-hydroxide-nitrate ZnO.

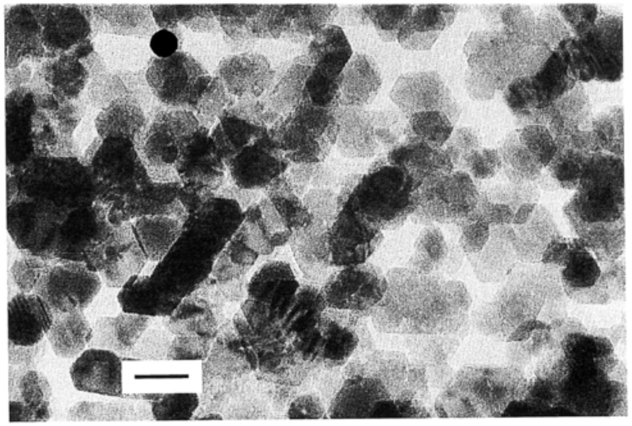

Fig. 28.9. TEM micrograph of ex-hydroxide-nitrate ZnO showing hexagonal crystallites (bar = 200 Å).

J. I. Langford, A. Boultif, J. P. Auffrédic, D. Louër, *J. Appl. Crystallogr.* 1993, 26, 22.

The Rietveld method

- Whole-pattern-fitting-structure refinement
- Least-squares refinement until the best fit is obtained of the entire powder pattern taken as the whole and the entire calculated pattern
- Simultaneously refined models of crystal structure(s), diffraction optics effects, instrumental factors and other specimen characteristics
- Feedback criteria during refinement
- Pattern decomposition and structure refinement are not separated steps

Procedures in Rietveld refinement

- Experimental data: numerical intensities y_i for each increment i in 2θ
- Simultaneous least-squares fit to all (thousands) of y_i
  - minimize $S_y = \Sigma_i \, y_i^{-1} (y_i - y_{ci})^2$
- Expression for y_{ci}

$$y_{ci} = s \, \Sigma_{hkl} \, L_{hkl} \, |F_{hkl}|^2 \, \Phi(2\theta_i - 2\theta_{hkl}) \, P_{hkl} \, A + y_{bi}$$

  - s: scale factor, L_{hkl} contains Lorentz polarization and multiplicity factors, Φ: profile function, P_{hkl} preferred orientation function, A: absorption factor, F_{hkl}: structure factor, y_{bi}: background intensity
- As in all non-linear least-squares refinements, false (local) minima may occur
- Good (near the global minimum) starting models are required

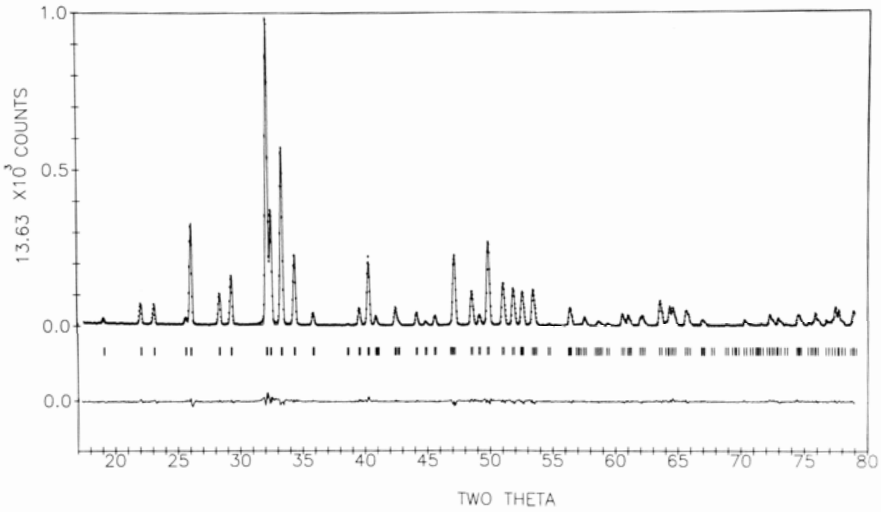

Fig. 1.1 Example of a Rietveld refinement plot. The specimen was fluorapatite. The observed intensity data, y_i, are plotted in the upper field as points with vertical error bars representing the counting statistical e.s.d.'s in them. The calculated pattern is shown in the same field as a solid-line curve. The difference, observed minus calculated, is shown in the lower field. The short vertical bars in the middle field indicate the positions of possible Bragg reflections.

Parameters in Rietveld refinement

- For each phase
  - x_j y_j z_j B_j N_j (Position, isotropic thermal parameter and site occupancy of the jth atom in the unit cell
  - Scale factor
  - Profile breadth parameters (2θ dependence of FWHM, typically Cagliotti function $FWHM^2 = U \tan^2\theta + V \tan\theta + W$)
  - Lattice parameters
  - Overall temperature factor
  - individual anisotropic temperature factors
  - Preferred orientation
  - Extinction
- Global parameters
  - 2θ-Zero
  - Instrumental profile (+ asymmetry)
  - Background (several parameters in analytical function)
  - Wavelength
  - Specimen displacement, transparancy
- Altogether some 10-100 parameters: Keep an eye on the refined parameters-to-reflections (independent observations) ratio to avoid over-fitting

Criteria of fit

- R-Bragg

$$R_B = \frac{\Sigma \,| I_K(\text{"}obs\text{"}) - I_K(calc) |}{\Sigma I_K(\text{"}obs\text{"})}$$

  - insensitive to misfits not involving the Bragg intensities of the phase(s) being modelled

- R weighted pattern

$$R_{wp} = \left(\frac{\Sigma w_i (y_i(obs) - y_i(calc))^2}{\Sigma w_i (y_i(obs))^2} \right)^{1/2}$$

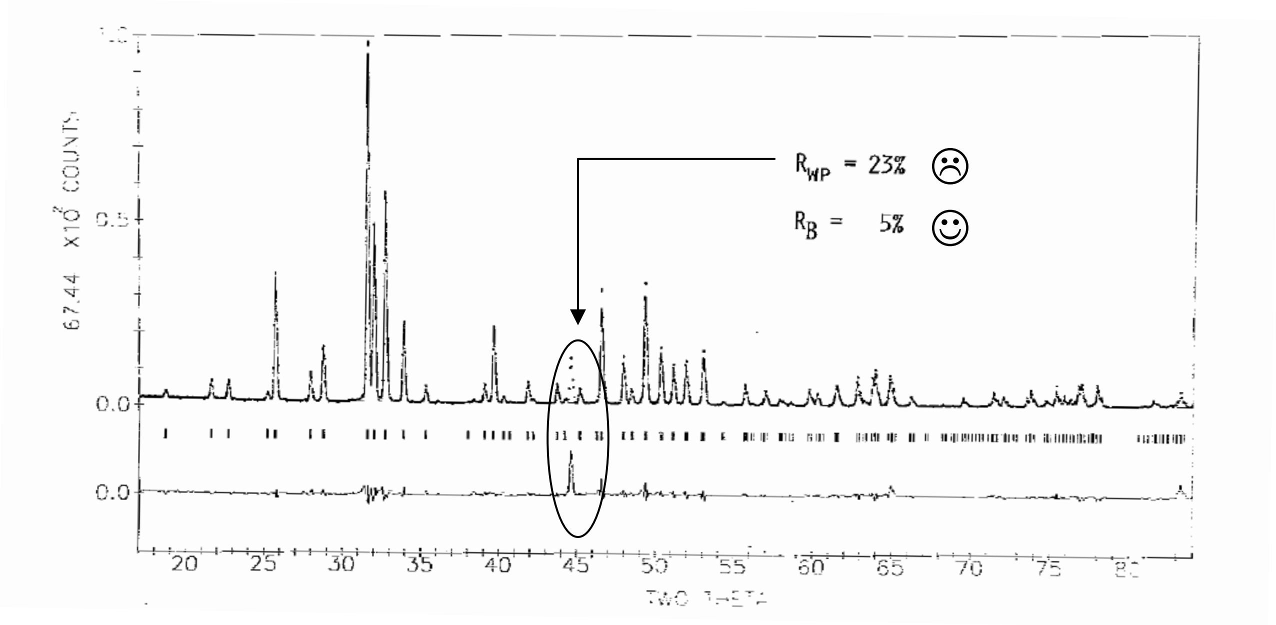

R_{WP} = 23% ☹

R_B = 5% ☺

Neutrons

- According to the wave-particle dualism ($\lambda = h/mv$, de Broglie) neutrons have wave properties
- As X-rays neutrons have a wavelength on the order of the atomic scale (Å) and a similar interaction strength with matter (penetration depth from µm to many cm)
- Neutrons generate interference patterns and can be used for Bragg diffraction experiments
- Same scattering theory for neutrons and X-rays

Generation of neutrons

- Neutron must be released from the atomic nuclei, two possibilities:
  - Fission reactor
    - ^{235}U nuclei break into lighter elements and liberate 2 to 3 neutrons for every fissioned element

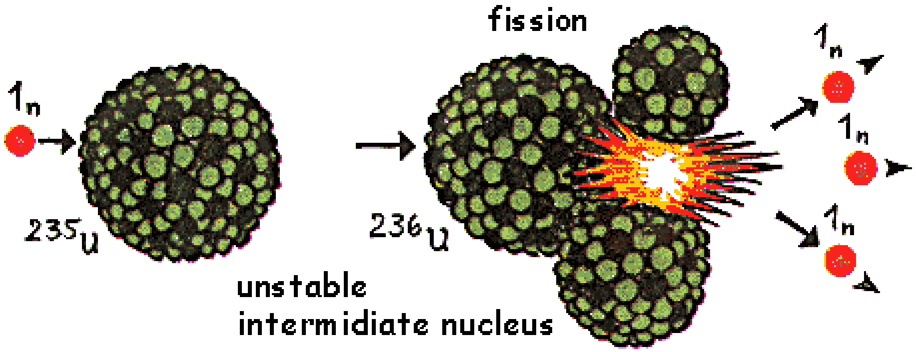

www.hmi.de

  - Spallation source
    - proton bombardment of lead nuclei, releasing spallation neutrons

Research reactor at Helmholtz Zentrum Berlin

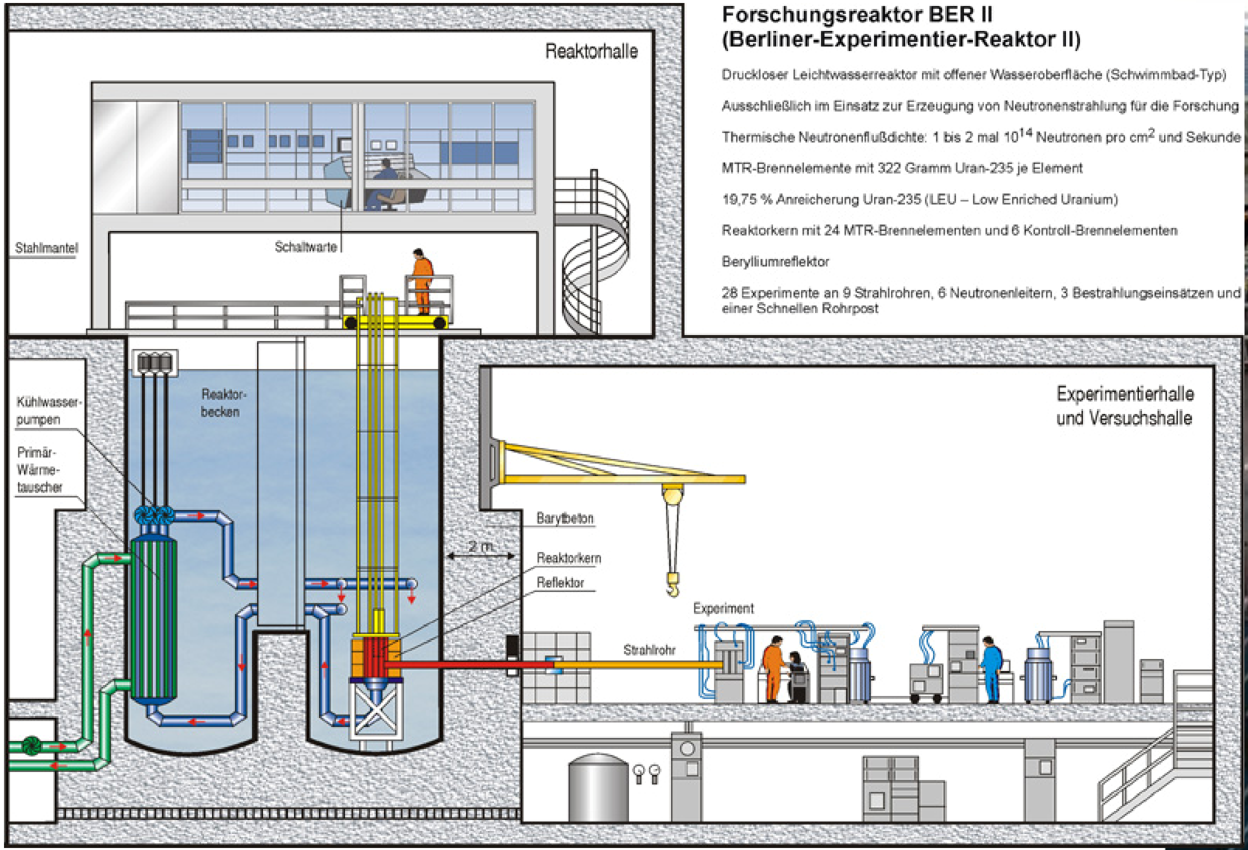

Forschungsreaktor BER II (Berliner-Experimentier-Reaktor II)

Druckloser Leichtwasserreaktor mit offener Wasseroberfläche (Schwimmbad-Typ)

Ausschließlich im Einsatz zur Erzeugung von Neutronenstrahlung für die Forschung

Thermische Neutronenflußdichte: 1 bis 2 mal 10^{14} Neutronen pro cm^2 und Sekunde

MTR-Brennelemente mit 322 Gramm Uran-235 je Element

19,75 % Anreicherung Uran-235 (LEU – Low Enriched Uranium)

Reaktorkern mit 24 MTR-Brennelementen und 6 Kontroll-Brennelementen

Berylliumreflektor

28 Experimente an 9 Strahlrohren, 6 Neutronenleitern, 3 Bestrahlungseinsätzen und einer Schnellen Rohrpost

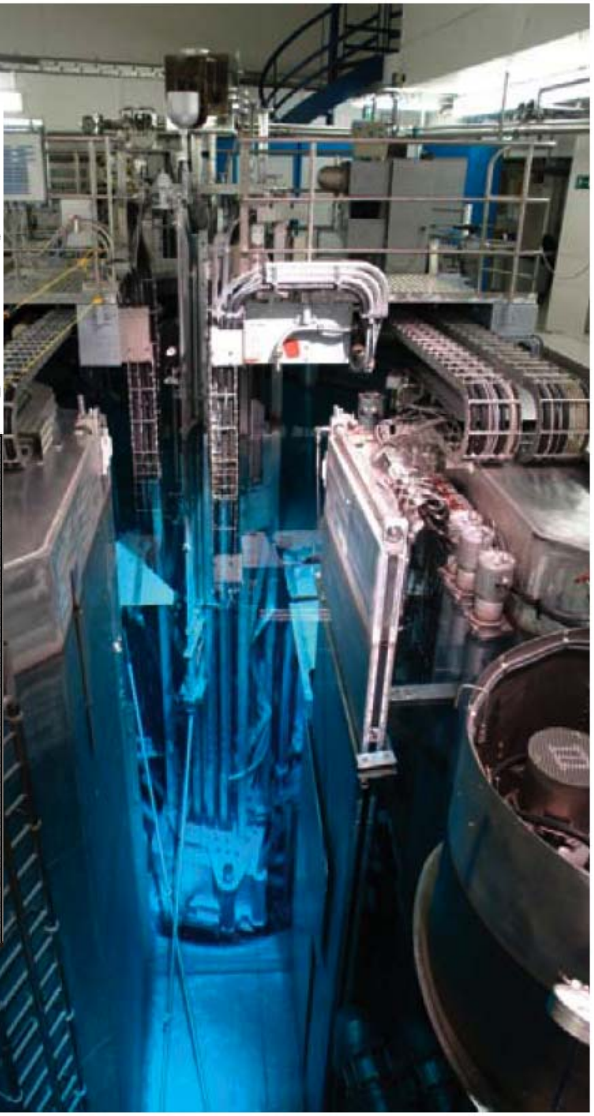

www.hmi.de

Research reactor at Helmholtz Zentrum Berlin

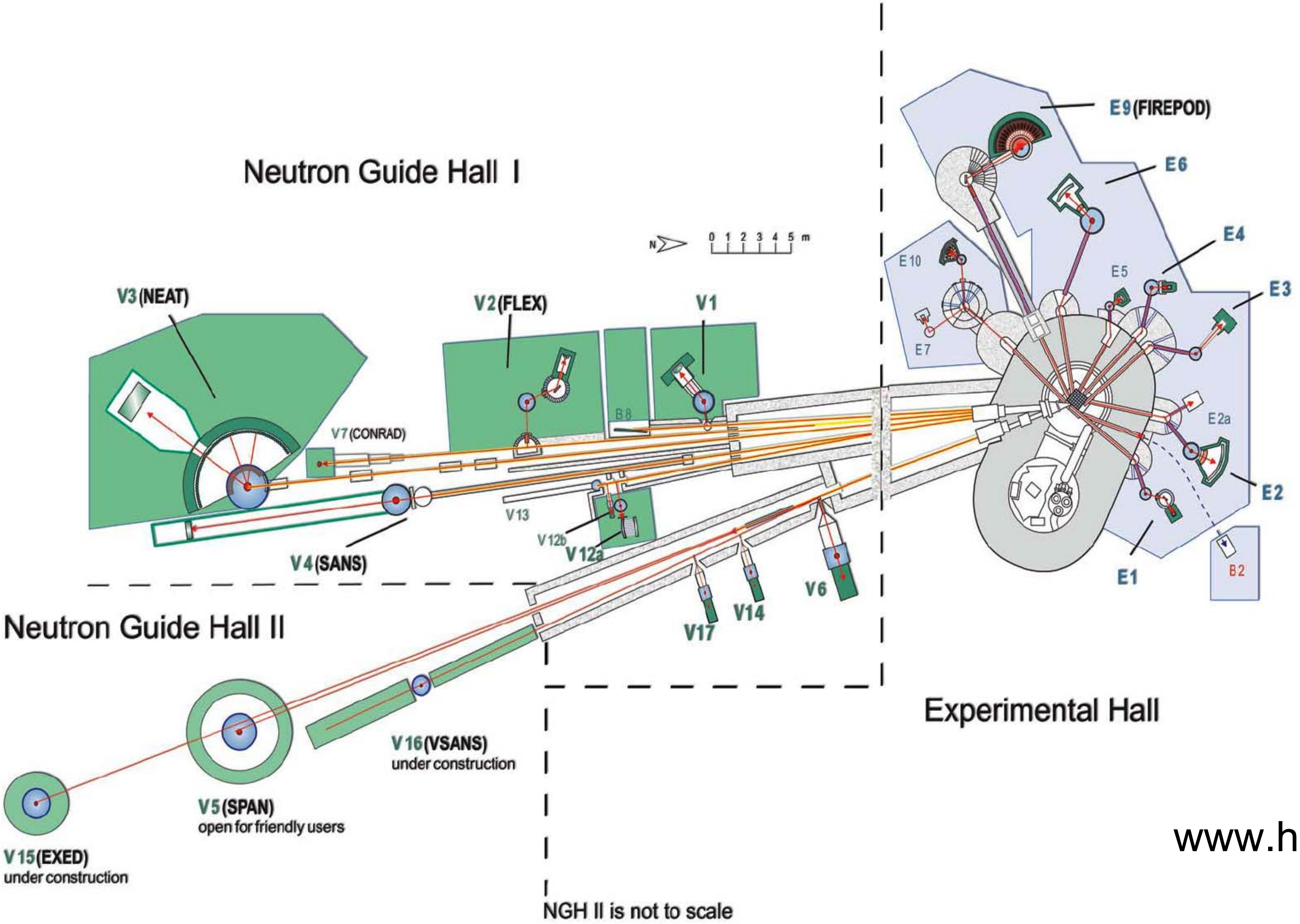

www.hmi.de

Properties of neutrons

- Fission process: 1 MeV – too high for practical use
- Neutrons are slowed down (moderated in water or carbon)
  - hot neutrons:
    - moderated at 2000°C
    - 0.1-0.5 eV, 0.3-1 Å, 10 000 m/s
  - thermal neutrons:
    - moderated at 40°C
    - 0.01-0.1 eV, 1-4 Å, 2000 m/s
  - cold neutrons:
    - moderated at -250°C
    - 0-0.01 eV, 0-30 Å, 200 m/s

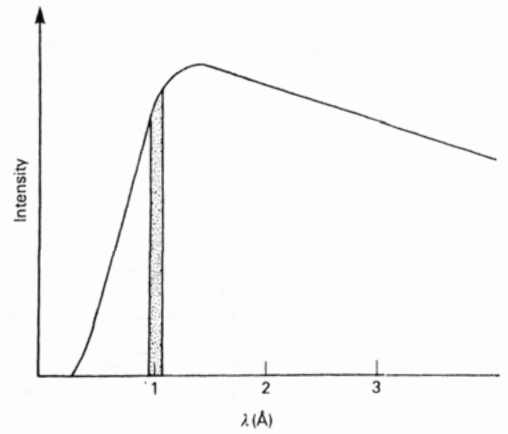

Fig. 2.16. Spectral distribution of moderated neutrons from a nuclear reactor. A narrow band of wavelengths can be selected for diffraction experiments.

Neutrons vs. X-rays

- Particle wave
- Mass, Spin 1/2, Magnetic dipole moment
- Neutrons interact with the nucleus
- Scattering power independent of 2θ

- Electromagnetic wave
- No mass, spin 1, no magnetic dipole moment
- X-ray photons interact with the electrons
- Scattering power falls off with 2θ

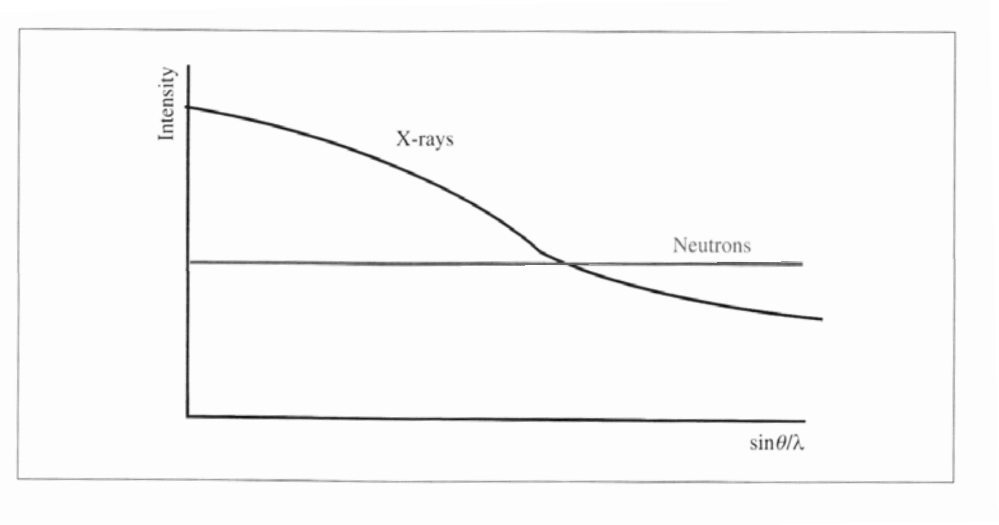

Figure 3.16 Variation of scattering amplitude with angle

Scattering lengths

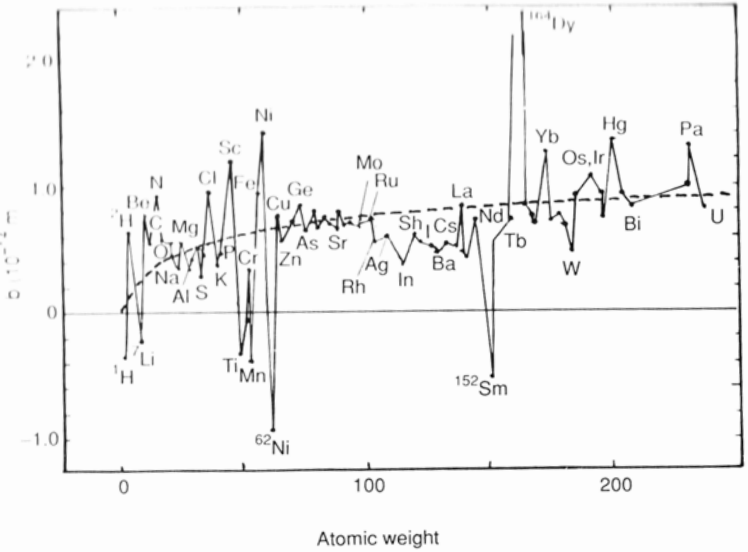

Fig. 1.3 Nuclear scattering lengths for thermal neutrons shown as a function of atomic weight. (Courtesy of Prof. H. Fuess.)

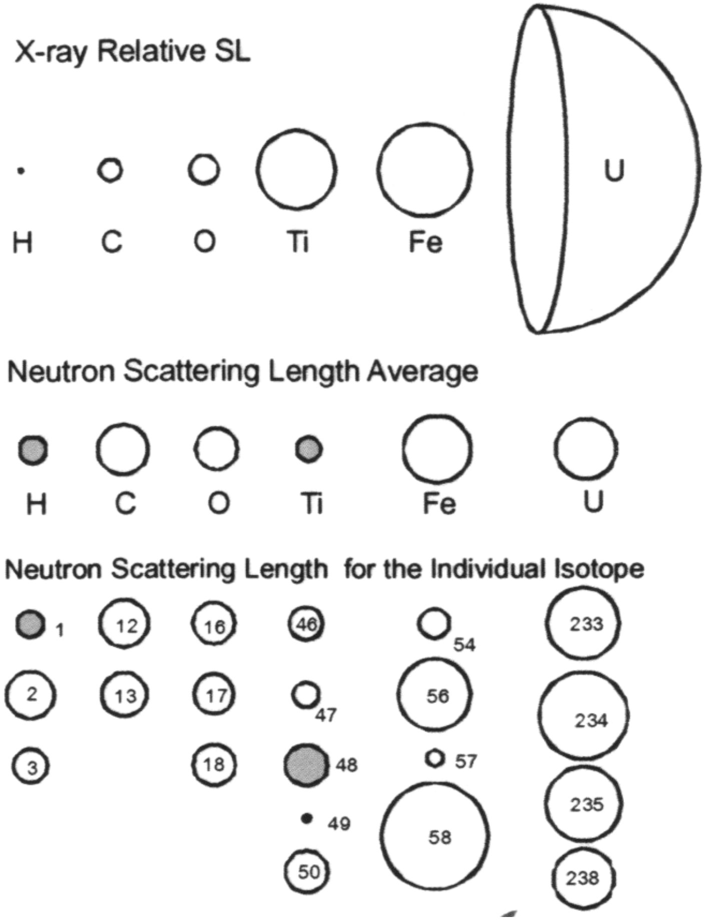

Neutron vs. XRD pattern

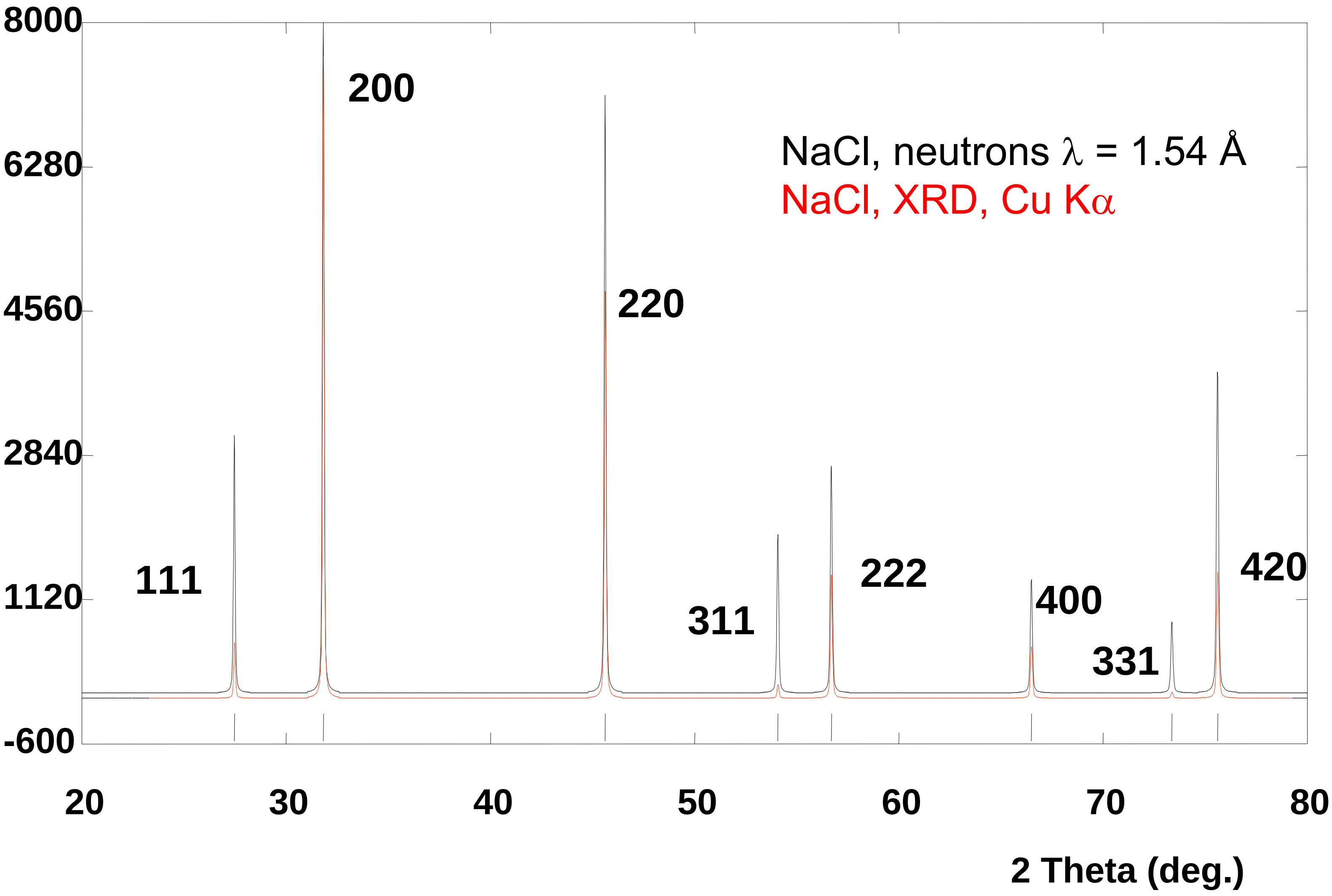

Neutrons vs. X-rays

- Lower absorption
- Large amounts of sample needed
- Neighbors and isotopes can be discriminated
- Light elements can be seen
- Low availability (nuclear reactor)
- Magnetic structures can be investigated
- Incoherent scatterers (eg. H) have to be avoided

- Stronger absorption
- Lower amounts of sample needed
- Neighbors and isotopes cannot be discriminated
- Light elements hard to detect
- High availability (lab instrument)

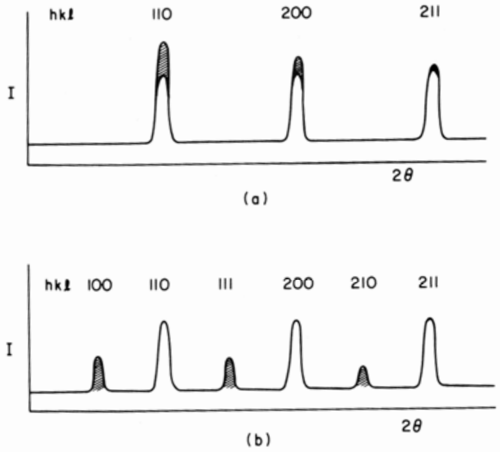

FIG. 4-27. Schematic neutron diffraction patterns from polycrystalline (a) bcc ferromagnet and (b) bcc antiferromagnet. The shaded area represents the contribution of the magnetic scattering which decreases with θ due to the decrease in magnetic scattering factor f_{mag}.

Application in catalysis

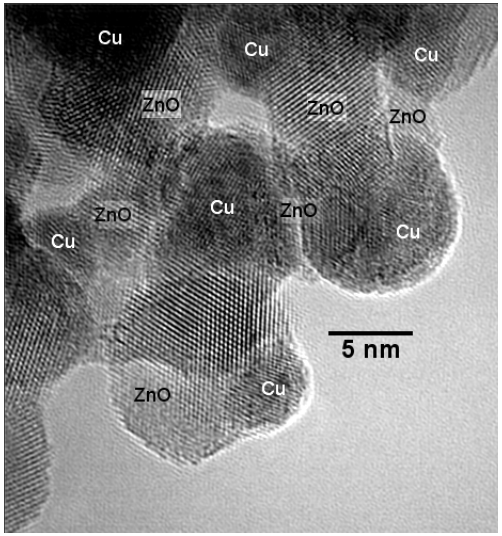

$Cu/ZnO/Al_2O_3$ catalysts for methanol synthesis

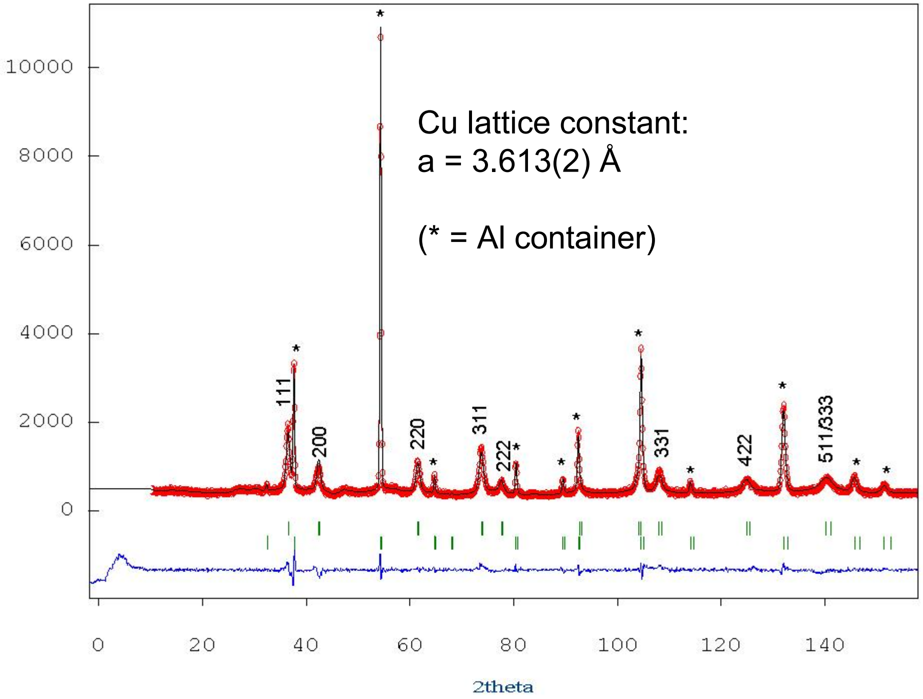

Cu lattice constant:
a = 3.613(2) Å

(* = Al container)

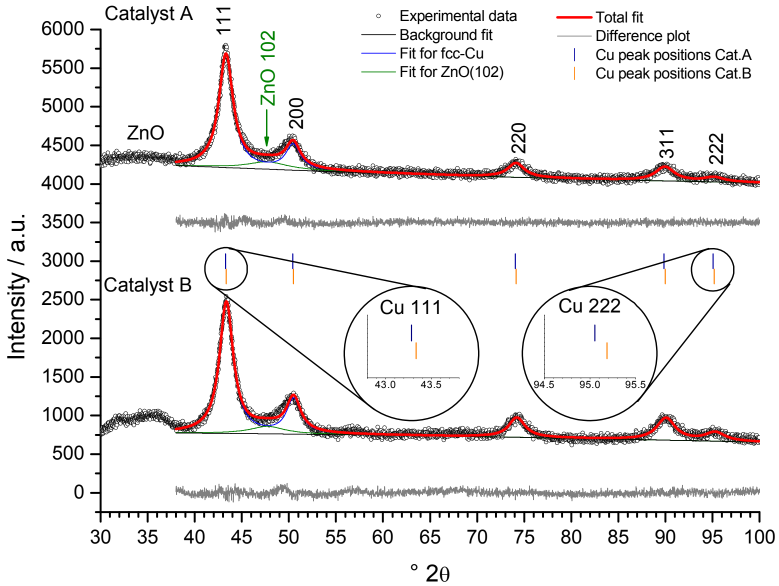

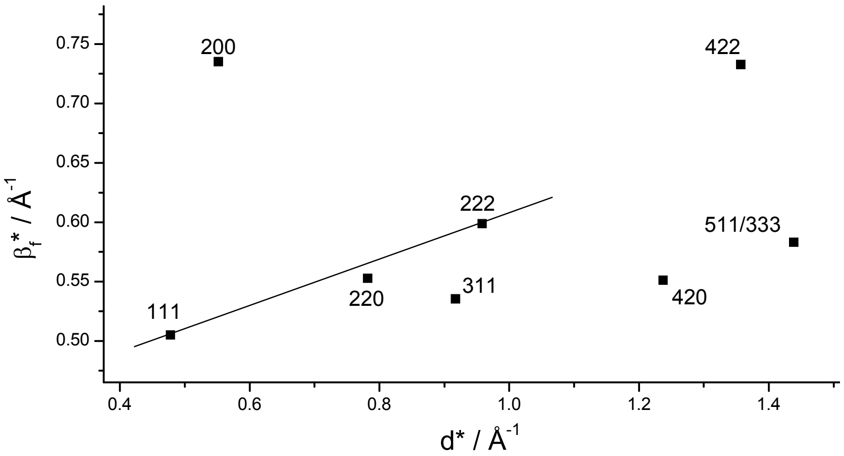

Summary

- Powder XRD can give information on crystalline phases (fingerprint), crystal structure and quantitative phase analysis (e.g. from Rietveld refinement) and size/strain effects (from line profile analysis)
- Neutron diffraction is a non-routine complementary technique allowing detection of light elements, recording of higher intensity Bragg reflections at high angle, discrimination of neighbouring elements

Literature / References

- L.H. Schwartz, J.B. Cohen “Diffraction from Materials” Academic Press, New York 1977.
- H.P. Klug, L.E. Alexander “X-Ray Diffraction Procedures” 2nd Edition, John Wiley, New York 1974.
- R.A. Yound (ed) “The Rietveld Method” IUCr, Oxford Science Publications, Oxford University Press 1993.
- S.E. Dann “Reaction and Characterization of Solids” RSC, Cambridge 2000.
- Educational material for the “Praktikum für Fortgeschrittene”, Institute of Inorganic Chemistry of the University Kiel.
- Helmhotz-Zentrum für Materialien und Energie: www.hmi.de.
- Handout “Weiterbildung Chemische Nanotechnologie”, Universität des Saarlands, Saarbrücken.
- Handout “Application of Neutrons and Synchroton Radiation in Engineering Material Science”, Virtual Institute Photon and Neutrons for Advanced Materials (PNAM).
- J. I. Langford, A. Boultif, J. P. Auffrédic, D. Louër, *J. Appl. Crystallogr.* 1993, 26, 22.
- F. Girgsdies: Lecture Series Modern Methods in Heterogeneous Catalysis: “X-Ray Diffraction in Catalysis” 2006.